III-nitride vertical hot electron transistor with polarization doping and collimated injection

Cite as: Appl. Phys. Lett. **121**, 223503 (2022); doi: 10.1063/5.0129920
Submitted: 7 October 2022 · Accepted: 12 November 2022 ·
Published Online: 29 November 2022

J. W. Daulton,[1,2,a)] R. J. Molnar,[1] J. A. Brinkerhoff,[1] M. A. Hollis,[1] and A. Zaslavsky[2]

AFFILIATIONS

[1]MIT Lincoln Laboratory, Lexington, Massachusetts 02142, USA
[2]School of Engineering, Brown University, Providence, Rhode Island 02912, USA

[a)]Author to whom correspondence should be addressed: Jeffrey_Daulton@brown.edu

ABSTRACT

III-nitride-based hot electron transistors (HETs) offer a significant promise as high-speed, high-power devices, but their performance has been limited to below that of competing technologies. Here, we report on a HET with current density $> 440\,\text{kA/cm}^2$ and common-emitter current gain >20. Polarization engineering of the emitter stack was used to allow for high-current collimated electron injection from the emitter with relatively low turn-on voltage. The use of only polarization charge in the undoped 10 nm-thick base allowed for high gain through minimization of scattering with atomic layer etching contact fabrication used to lower base access resistance.

Published under an exclusive license by AIP Publishing. https://doi.org/10.1063/5.0129920

In recent years, GaN HEMTs have become the primary technological solution for most high-power, high-frequency applications. However, for mm-wave-THz applications, InP heterojunction bipolar transistors (HBTs) have remained the dominant technology due to very high current density and good linearity, resulting in devices performing very close to their theoretical limits. While GaN has many favorable material properties compared to InP, including higher thermal conductivity, higher critical field, and lower dielectric constant, poor hole mobility and difficulties with effective *p*-type doping have hindered the development of III-nitride-based HBTs.[1]

Research in the 1980s using the III-As material system demonstrated the possibility of an all-electron analog to the HBT, where the conventional electron–hole carrier types were replaced with hot (energetic) and cold (thermalized) electron populations. In the hot-electron transistor (HET), energetic electrons traverse a narrow quantum well base populated with cold electrons and are collected over the base-collector barrier. In principle, given a sufficiently long hot-electron mean-free path, the HET obviates the carrier transit time limitation on the device speed, leaving only parasitic limits.[2,3] Ultimately, the III-As HET work was limited by low injection energies (due to small Γ–L valley energy separation of GaAs) and difficulties with contact formation to narrow base layers.[3,4] Recent work has recognized the value of revisiting the HET concept in GaN, where the (Γ to M–L) valley energy separation is $> 6\times$ larger than in GaAs. GaN-based HETs incorporating base doping resulted in working devices with reasonable current density but relatively low gain due to impurity scattering in the base.[5,6] Alternatively, the demonstration of the GaAs induced base transistor[7] without base doping (and hence impurity scattering) led to a similar solution for GaN, taking advantage of the high-mobility 2D electron gas (2DEG) that forms spontaneously in AlGaN/GaN heterostructures.[8] However, the resulting devices suffered from relatively low current density and gain,[9] though the gain improved when the base thickness was reduced.[10,11]

In this Letter, we present a III-N HET device combining a narrow 10 nm polarization-doped 2DEG-containing GaN base contacted by a selective low-damage BCl_3/O_2 atomic layer etching (ALE) process[12] together with a quantum well emitter that provides collimated electron injection into the base. The resulting near-perpendicular transport mitigates gain degradation due to broad electron energy and incident angle distribution, analogous to Landau damping in collisionless plasmas.[13] It also reduces plasmon coupling[2] and probability of phonon emission,[14] leading to a measured common-emitter current gain $\beta > 20$ and high collector current density $J_C > 440\,\text{kA/cm}^2$.

The epitaxial structure of the transistor is shown in Fig. 1(a), including the Al content of the AlGaN layers and the donor doping density. It is grown by MOCVD on a 2 in. sapphire substrate with a 4 μm GaN buffer and an estimated dislocation density of $\sim 5 \times 10^8\,\text{cm}^{-2}$, as measured by AFM. The emitter stack consists of a highly doped ($\sim 10^{19}\,\text{cm}^{-3}$, near the practical limit for efficient Si doping in GaN) emitter cap for the formation of a low-resistance contact, with a triangular quantum well formed by polarization fields at the interface of the graded AlGaN emitter and an ultrathin 1.5 nm AlN

Published under an exclusive license by AIP Publishing

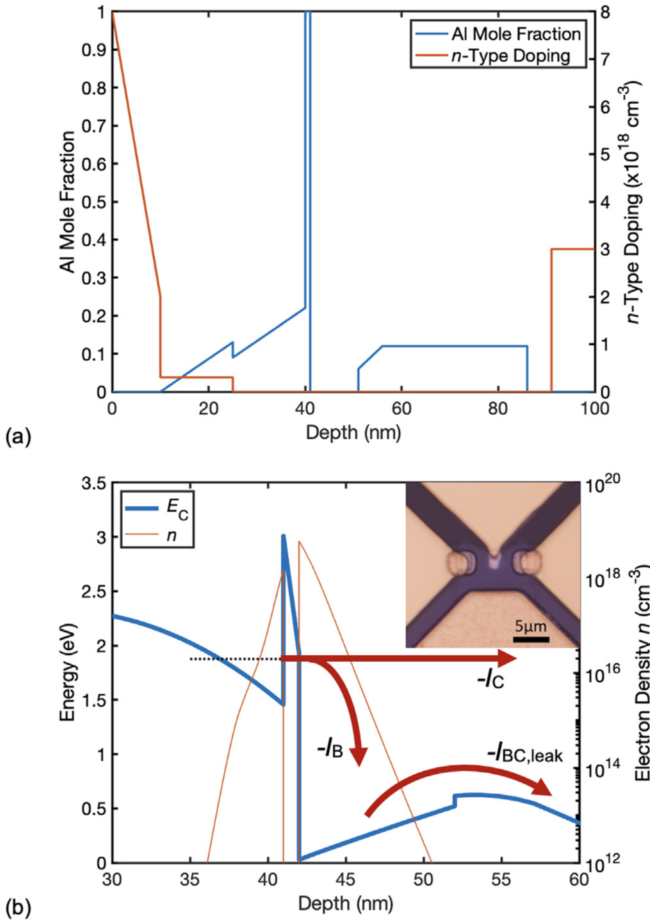

FIG. 1. (a) Device structure with Al mole fraction and doping profile. (b) Self-consistent emitter-base conduction band diagram (blue) at $V_{BE} = 2$ V and $V_{CB} = 2$ V, showing electron density (orange), the lowest subband in the emitter (dotted line), and major electron flow components (red arrows). The inset shows top-view photograph of the device.

tunneling barrier. The narrow 10 nm undoped GaN base was designed to contain a 2DEG density of $\sim 3.5 \times 10^{12}$ cm^{-2}, whereas the collector region consists of a graded AlGaN base-collector transition layer to minimize carrier reflection off the $Al_{0.12}Ga_{0.88}N$ collector, a strategy employed in GaAs-based devices to reduce reflection from an abrupt barrier.[15] The resulting conduction band diagram is illustrated in Fig. 1(b) under operating bias conditions ($V_{BE} = 2$ V and $V_{CB} = 2$ V), including the energy of the lowest quantized subband in the emitter, together with the predicted electron density in the emitter and base obtained from a self-consistent technology computer-aided design (TCAD) simulation,[16] as well as the electron current flow components. The inset in Fig. 1(b) shows a top-view photograph of the device.

Fabrication of the transistor structure involved first isolating the active mesa by etching through the AlN tunnel barrier, eliminating the base 2DEG outside the device mesa. Base contacts are formed as sidewall contacts to the 2DEG, with base etching accomplished by an ALE process with thermal desorption of reaction products,[12] without any damaging ion bombardment. A metal stack of Ti/Al/Pt is then deposited by Ar sputtering for both base and collector contacts, which are subsequently annealed at 550 °C in forming gas. The emitter contact metal of Ti/Pt/Au/Pt is subsequently deposited, bridging over a layer of PECVD SiO_2 at the mesa edge to avoid electrical contact to the device sidewall. This SiO_2 dielectric layer also extends beyond the physical extent of the probe pads to eliminate the possibility of leakage currents outside the device mesa. The emitter metal is subsequently annealed at 400 °C in forming gas, and a final pad metal of Ti/Pt/Au is deposited before the n^+-GaN emitter cap is removed with the same BCl_3/O_2 ALE process. A cross-sectional schematic of the device (with only one base contact shown) and the cross-sectional TEM of the sidewall contact are shown in the insets of Fig. 2(a).

Figure 2(a) presents the base-to-base $I(V)$ between the two base contacts (separated by $\sim 7\,\mu$m), before and after the n^+-GaN emitter cap etch. Prior to the cap etch, in-process transfer length method (TLM) measurements estimated contact resistance $R_C \sim 0.7$ Ω·mm and 2DEG per-square resistance of ~ 800 Ω. This sheet resistance is in good agreement with the simulated 2DEG density of $\sim 3.5 \times 10^{12}$ cm^{-2} and electron mobility of ~ 2200 cm^2/V·s, a value obtained from previous Hall effect measurements on GaN HEMT structures grown by similar techniques.[17] The partial cap etch between the metal emitter and base contacts was intended to deplete the mobile carriers in the cap without exposing any AlGaN layers (to avoid Fermi level pinning on surface defects). As can be seen in Fig. 2(a), the cap etch went too deep, increasing the base-to-base resistance markedly, but still leading to high-performance devices.

Turning to the HET transistor with a $\sim 1.1 \times 1.2\,\mu$m^2 emitter contact and $\sim 3\,\mu$m emitter edge to base contact separation, Figs. 2(b) and 2(c) show the emitter-base and base-collector diode measurements, with the other terminal floating. The emitter-base diode in Fig. 2(b) shows good rectification, with the onset of significant current at approximately $V_{BE} = 0.7$ V and a current density exceeding 5 mA/μm at $V_{BE} = 4$ V. The collector-base diode in Fig. 2(c) also shows rectification, with thermionic current at large $V_{CB} > 2$ V [the normal mode of HET operation, see Fig. 1(b)], agreeing with TCAD simulation shown by the orange line, but considerably larger leakage for lower $0 < V_{CB} < 2$ V. As discussed below, this added leakage, which we attribute to dislocations, complicates the extraction of common-emitter β at high V_{CB}.[9,10]

The Gummel characteristics are shown in Fig. 3, with a peak Gummel $\beta \sim 2$ and a peak transconductance (dI_C/dV_{BE}) of 310 kS/cm^2 at $V_{BE} = 4$ V. The increasing gain with larger V_{BE} is a function of increased injection energy, which leads to more likely ballistic transport across the base and over the collector barrier. Intervalley electron transfer resulting from injection of electrons above the Γ to M–L energy separation would be expected to result in the degradation of gain at higher V_{BE}, but no sharp reduction in Gummel β is observed.

The common-emitter HET characteristics as a function of V_{CE} for $V_{BE} = 1$–4 V are shown in Fig. 4(a). Increased collector current at large V_{CB} values is expected because of lowered collector barrier [see Fig. 1(b)], as this allows for increased collection probability of injected hot electrons that have experienced scattering events in the base. Common-emitter gain of >75 at $V_{BE} = 1.5$ V and >55 at $V_{BE} = 2$ V is observed in Fig. 4(b), after correcting for the collector-base leakage current $I_{BC,leak}$ by subtracting $I_{BC,leak}$ measured in Fig. 2(c) from I_C and adding it to I_B, $\beta = (I_C - I_{BC,leak})/(I_B + I_{BC,leak})$. This correction avoids artificially inflating the gain when the collector-base leakage current becomes comparable to the true base current.[9,10] Further

Published under an exclusive license by AIP Publishing

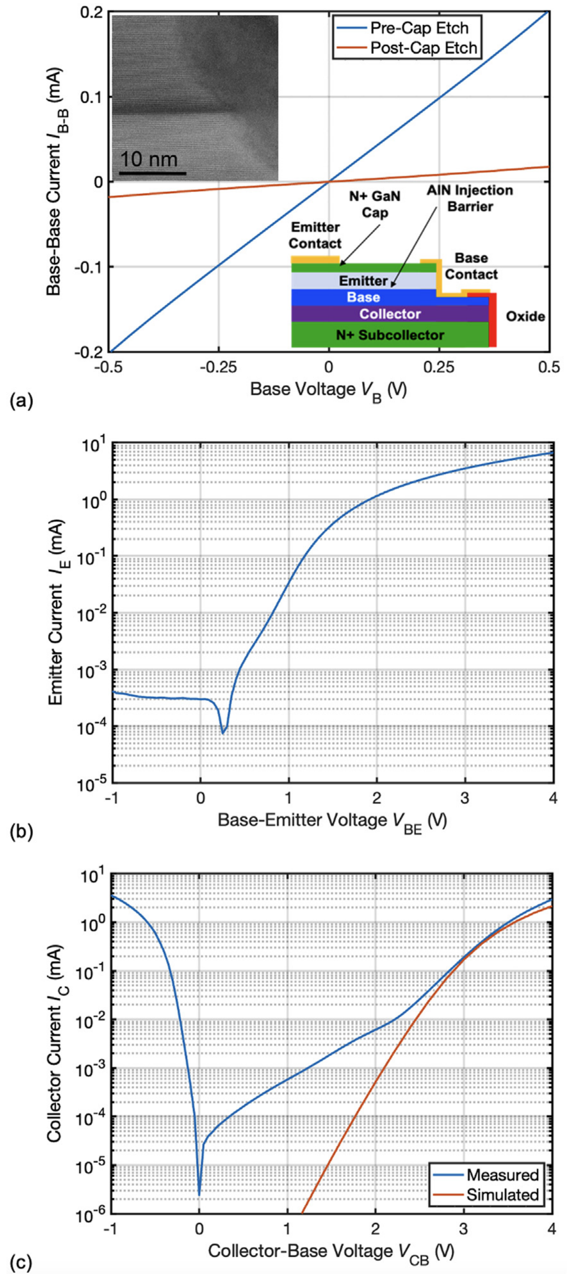

FIG. 2. (a) Base-to-base $I(V)$ between the two base contacts, before and after the GaN cap etch. The insets show a cross-sectional dark-field (DF) TEM of the sidewall base contact and a schematic cross section of the device (the second symmetric base contact is not shown). Emitter-base (b) and base-collector (c) characteristics, with the third terminal floating. The orange line in (c) indicates the TCAD-simulated thermionic emission base-collector current.

restricting these gain values in Fig. 4(b) with the condition that $I_{BC,leak} < 0.1 I_B$ results in common-emitter gain of >10 at $V_{BE} = 1.5$ V and >22 at $V_{BE} = 2$ V—the transition is marked in Fig. 4(b). The collector current density at $V_{CE} = V_{BE} = 4$ V reaches 440 kA/cm^2, comparable to

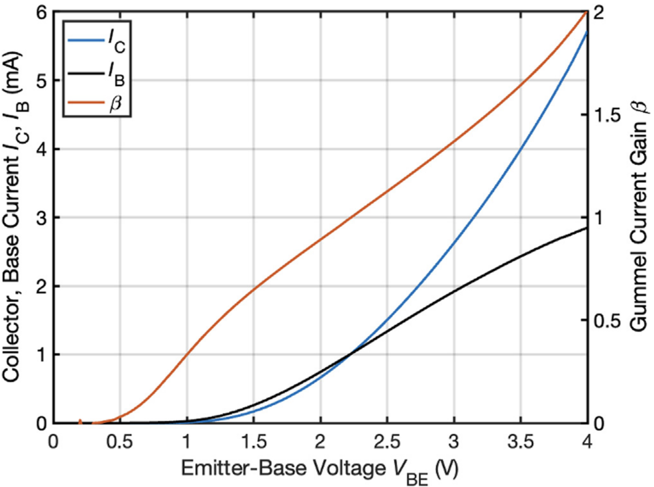

FIG. 3. Gummel plot showing I_C, I_B, and Gummel current gain β as a function of V_{BE} (emitter area is 1.3 μm^2).

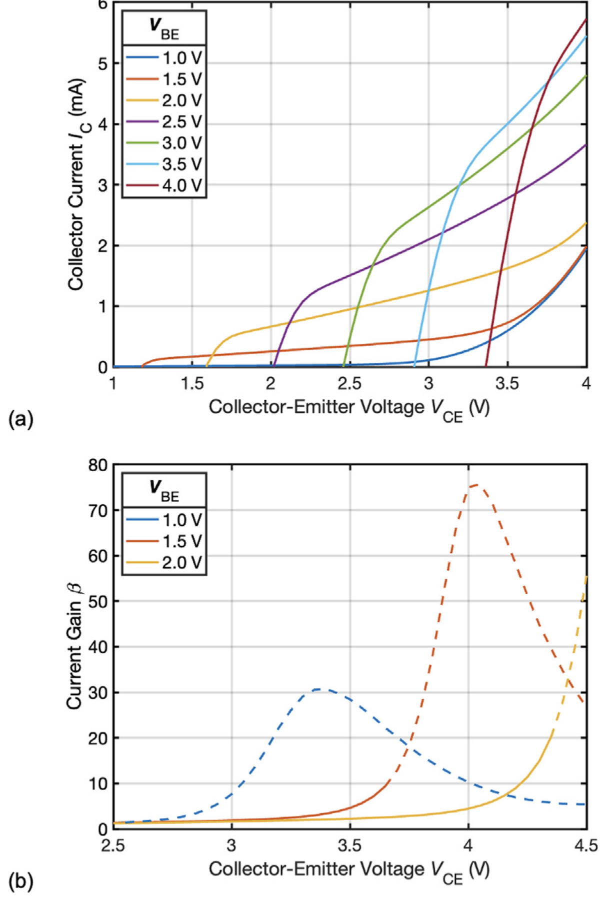

FIG. 4. (a) Common-emitter characteristics for $V_{BE} = 1$ to 4 V as a function of V_{CE} and (b) common-emitter current gain β vs V_{CE} (obtained after removing the contribution of base-collector leakage) and the dashed lines show β for $I_{BC,leak} > 0.1 I_B$.

Published under an exclusive license by AIP Publishing

TABLE I. Figures of merit for GaN-based HETs.

Paper	$J_{C,max}$	$g_{m,max}$	Gummel β	Common-emitter β
Gupta[9]	2.5 kA/cm^2	⋯	⋯	1.02
Yang[5]	62.2 kA/cm^2	12.4 kS/cm^2	1.5	⋯
Yang[6]	46.6 kA/cm^2	30 kS/cm^2	⋯	14.5
Gupta[11]	2.7 kA/cm^2	⋯	3.5	3.5
This work	440 kA/cm^2	310 kS/cm^2	2	>20

the highest-performance InP-based HBTs.[18] High base current, from the combination of high emitter current density and limited gain, results in a substantial voltage drop over the base access region, decreasing effective V_{BE} at the edge of the emitter-base junction. Simulations indicate significant emitter current crowding, as is typical of HBTs, so the performance could be improved by fabricating a narrower emitter stripe.

A comparison of our results to previously reported nitride-based HETs is summarized in Table I. We observe higher common-emitter β, current density, and transconductance, despite increased base access resistance due to excessive emitter cap etch and emitter-base current leakage resulting in low-energy electron injection that cannot surmount the collector barrier at $V_{CB} < 2$ V, which we attribute to dislocations, rather than other processes such as sidewall leakage.

In addition to miniaturizing the dimensions of the transistor, as in high-performance HBTs, an obvious avenue toward higher performance is a reduction in the dislocation density. Conductive dislocations in III-N materials have been shown to exhibit a variety of mid-gap energies,[19,20] leading to parasitic leakage currents that limit the current gain. These dislocations have also been shown to induce 2DEG nonuniformity, resulting in significant vertical field inhomogeneity.[21] In the context of hot electron injection of Fig. 1(b), these leakage currents may come in the form of electrons being injected into the base from below the emitter conduction band, broadening the injected electron distribution, which is not readily distinguishable from scattering within the base region. As the injection energy of electrons coming from dislocations is below the base-collector barrier, such electrons will necessarily contribute to base current, lowering the measured current gain and artificially increasing the apparent scattering rate. Similarly, such dislocations within the base-collector barrier result in increased base-collector leakage evident in Fig. 2(c), further complicating the extraction of common-emitter current gain. The use of bulk substrates, with $\sim 10^6$ cm^{-2} dislocation densities,[5,6,19] would reduce the average dislocation count in a $\sim 1\ \mu$m^2 emitter area to less than 1, eliminating these mid-gap states and allowing clearer determination of the contribution of base scattering. The resulting increased β would reduce voltage drop over the extrinsic base region and increase the collector current. Improved thermal conductivity from bulk substrates compared to heteroepitaxial growth[22] would also likely improve current density of the device.

In conclusion, we have fabricated and characterized GaN-based HETs with electron injection from a 2D subband in the emitter and good Ohmic contacts to a narrow, polarization-doped GaN base. The observed collector current density reaches ~ 440 kA/cm^2 and the common-emitter gain reaches a peak value of >20 when a strict constraint for collector-base leakage current is imposed. Future work will include the extraction of injection energy spread by operating the device as a ballistic electron spectrometer at cryogenic temperatures as well as fabrication of similar designs on bulk GaN substrates to reduce dislocation-induced leakage and miniaturizing the emitter strip width and base-emitter contact separation.

DISTRIBUTION STATEMENT A. Approved for public release. Distribution is unlimited. upported by the Under Secretary of Defense for Research and Engineering under Air Force Contract No. FA8702-15-D-0001. Any opinions, findings, conclusions or recommendations expressed in this material are those of the author(s) and do not necessarily reflect the views of the Under Secretary of Defense for Research and Engineering. The lead author acknowledges the support of the Lincoln Scholars Program during his Brown Ph.D. studies. The authors would like to thank G. W. Turner for useful discussions.

AUTHOR DECLARATIONS

Conflict of Interest

The authors have no conflicts to disclose.

Author Contributions

Jeffrey W. Daulton: Conceptualization (equal); Data curation (lead); Formal analysis (lead); Funding acquisition (lead); Investigation (lead); Methodology (equal); Project administration (lead); Resources (lead); Writing – original draft (lead); Writing – review & editing (equal). **Richard J. Molnar:** Investigation (supporting); Methodology (equal); Resources (equal). **Jan A. Brinkerhoff:** Investigation (supporting); Methodology (supporting); Resources (supporting). **Mark A. Hollis:** Conceptualization (supporting); Formal analysis (equal); Investigation (supporting); Methodology (supporting); Project administration (equal); Supervision (equal); Writing – review & editing (equal). **Alexander Zaslavsky:** Conceptualization (equal); Methodology (equal); Project administration (equal); Supervision (equal); Writing – review & editing (equal).

DATA AVAILABILITY

The data that support the findings of this study are available from the corresponding author upon reasonable request.

REFERENCES

[1] L. Zhang, Z. Cheng, J. Zeng, H. Lu, L. Jia, Y. Ai, and Y. Zhang, "AlGaN/GaN heterojunction bipolar transistor with selective-area grown emitter and improved base contact," IEEE Trans. Electron Devices **66**, 1197 (2019).
[2] M. Heiblum, D. C. Thomas, C. M. Knoedler, and M. I. Nathan, "Tunneling hot-electron transfer amplifier: A hot-electron GaAs device with current gain," Appl. Phys. Lett. **47**, 1105 (1985).
[3] M. A. Hollis, S. C. Palmateer, L. F. Eastman, N. V. Dandekar, and P. M. Smith, "Importance of electron scattering with coupled plasmon-optical phonon modes in GaAs planar-doped barrier transistors," IEEE Electron Device Lett. **4**, 440 (1983).
[4] M. Heiblum, E. Calleja, I. M. Anderson, W. P. Dumke, C. M. Knoedler, and L. Osterling, "Evidence of hot-electron transfer into an upper valley in GaAs," Phys. Rev. Lett. **56**, 2854 (1986).

Published under an exclusive license by AIP Publishing

[5]Z. C. Yang, Y. Zhang, D. N. Nath, J. B. Khurgin, and S. Rajan, "Current gain in sub-10 nm base GaN tunneling hot electron transistors with AlN emitter barrier," Appl. Phys. Lett. **106**, 032101 (2015).
[6]Z. C. Yang, Y. Zhang, S. Krishnamoorthy, D. N. Nath, J. B. Khurgin, and S. Rajan, "Current gain above 10 in sub-10 nm base III-nitride tunneling hot electron transistors with GaN/AlN emitter," Appl. Phys. Lett. **108**, 192101 (2016).
[7]C.-Y. Chang, W. C. Lu, M. S. Jame, Y. H. Wang, S. Luryi, and S. M. Sze, "Induced base transistor fabricated by molecular beam epitaxy," IEEE Electron Device Lett. **7**, 497 (1986).
[8]M. S. Shur, A. D. Bykhovski, R. Gaska, M. A. Khan, and J. W. Wang, "AlGaN-GaN-AlInGaN induced base transistor," Appl. Phys. Lett. **76**, 3298 (2000).
[9]G. Gupta, M. Laurent, H. Li, D. J. Suntrup III, E. Acuna, S. Keller, and U. K. Mishra, "Design space of III-N hot electron transistors using AlGaN and InGaN polarization-dipole barriers," IEEE Electron Device Lett. **36**, 23 (2015).
[10]G. Gupta, E. Ahmadi, K. Hestroffer, E. Acuna, and U. K. Mishra, "Common emitter current gain >1 in III-N hot electron transistors with 7-nm GaN/InGaN base," IEEE Electron Device Lett. **36**, 439 (2015).
[11]G. Gupta, E. Ahmadi, D. J. Suntrup III, and U. K. Mishra, "Establishment of design space for high current gain in III-N hot electron transistors," Semicond. Sci. Technol. **33**, 015018 (2018).
[12]J. W. Daulton, R. J. Molnar, and D. M. Lennon, "Selectivity control in AlGaN/GaN atomic layer etching," in AVS Atomic Layer Etching Workshop (2015).
[13]A. A. Grinberg and S. Luryi, "Ballistic versus diffusive base transport in the high-frequency characteristics of bipolar transistors," Appl. Phys. Lett. **60**, 2770 (1992).
[14]R. J. E. Jansen, B. Farid, and M. J. Kelly, "Perpendicular electron transport through a two-dimensional electron-gas layer," Appl. Phys. Lett. **60**, 1881 (1992).
[15]A. F. J. Levi and T. H. Chiu, "Room-temperature operation of hot-electron transistors," Appl. Phys. Lett. **51**, 984 (1987).
[16]See https://www.synopsys.com/silicon/tcad/device-simulation/sentaurus-device.html Synopsys Sentaurus Version 2019.02 (2019).
[17]S. Warnock, S.-L. Chen, J. Knecht, R. Molnar, D.-R. Yost, M. Cook *et al.*, "InAlN/GaN-on-Si HEMT with 4.5 W/mm in a 200-mm CMOS-compatible MMIC process for 3D integration," in *2020 IEEE/MTT-S International Microwave Symposium (IMS)* (IEEE, 2020), pp. 289–292.
[18]Z. Griffith, "50–250 GHz power amplifier MMICs: Design, status and opportunities using a 250-nm InP HBT technology," in IEEE MTT-S Webinar (2020).
[19]P. Kozodoy, J. P. Ibbetson, H. Marchand, P. T. Fini, S. Keller, J. S. Speck, S. P. DenBaars, and U. K. Mishra, "Electrical characterization of GaN p-n junctions with and without threading dislocations," Appl. Phys. Lett. **73**, 975 (1998).
[20]H. Zhang, E. J. Miller, and E. T. Yu, "Analysis of leakage current mechanisms in Schottky contacts to GaN and AlGaN/GaN grown by molecular beam epitaxy," J. Appl. Phys. **99**, 023703 (2006).
[21]M. Wohlfahrt, M. J. Uren, Y. Yin, K. B. Lee, and M. Kuball, "Vertical field inhomogeneity associated with threading dislocations in GaN high electron mobility transistor epitaxial stacks," Appl. Phys. Lett. **119**, 243502 (2021).
[22]T. E. Beechem, A. E. McDonald, E. J. Fuller, A. A. Talin, C. M. Rost, J.-P. Maria, J. T. Gaskins, P. E. Hopkins, and A. A. Allerman, "Size dictated thermal conductivity of GaN," J. Appl. Phys. **120**, 095104 (2016).

Published under an exclusive license by AIP Publishing